Regulator of G protein signalling 18 promotes osteocyte proliferation by activating the extracellular signal-regulated kinase signalling pathway

YONG MENG[1,2], SI-QIANG QIU[3], QIANG WANG[3] and JIN-LIANG ZUO[3]

[1]Department of Orthopaedics, The Fifth Affiliated Hospital Jinan University, Heyuan, Guangdong 517000;
[2]Department of Orthopaedics, Central People's Hospital of Zhanjiang, Zhanjiang, Guangdong 524000;
[3]Department of Spine Surgery, The Fourth People's Hospital of Jinan, Jinan, Shandong 250031, P.R. China

Abstract. Osteocyte function is critical for metabolism, remodelling and regeneration of bone tissue. In the present study, the roles of regulator of G protein signalling 18 (RGS18) were assessed in the regulation of osteocyte proliferation and bone formation. Target genes and signalling pathways were screened using the Gene Expression Omnibus (GEO) database and Gene Set Enrichment Analysis (GSEA). The function of RGS18 and the associated mechanisms were analysed by Cell Counting Kit 8 assay, 5-ethynyl-2'-deoxyuridine assay, flow cytometry, reverse transcription-quantitative PCR, western blotting and immunostaining. Overlap analysis of acutely injured subjects (AIS) and healthy volunteers (HVs) from the GSE93138 and GSE93215 datasets of the GEO database identified four genes: *KIAA0825*, *ANXA3*, *RGS18* and *LIPN*. Notably, *RGS18* was more highly expressed in peripheral blood samples from AIS than in those from HVs. Furthermore, *RGS18* overexpression promoted MLO-Y4 and MC3T3-E1 cell viability, proliferation and S-phase arrest, but inhibited apoptosis by suppressing caspase-3/9 cleavage. Silencing *RGS18* exerted the opposite effects. GSEA of GSE93138 revealed that RGS18 has the ability to regulate MAPK signalling. Treatment with the MEK1/2 inhibitor PD98059 reversed the *RGS18* overexpression-induced osteocyte proliferation, and treatment with the ERK1/2 activator 12-O-tetradecanoylphorbol-13-acetate reversed the effects of *RGS18* silencing on osteocyte proliferation. In conclusion, RGS18 may contribute to osteocyte proliferation and bone fracture healing via activation of ERK signalling.

Correspondence to: Professor Yong Meng, Department of Orthopaedics, The Fifth Affiliated Hospital Jinan University, 892 Donghuan Road, Heyuan, Guangdong 517000, P.R. China
E-mail: masonmed@tom.com

Introduction

Bone fractures are common traumatic injuries of the bone cortex (1). Fracture healing is a regenerative process that recapitulates a number of the ontological events of embryonic skeletal development (1,2). Bone fracture healing is histologically defined in four steps: The initial inflammation-responsive phase within the first several days after fracture, the generation of surrounding soft callus and subsequent hard callus formation, followed by the osteoblast-induced formation of woven bone on the calcified matrix and recreation of the appropriate anatomical shape (2). The mechanisms involved in fracture healing are highly complex and are closely related to the interplay between cells, the extracellular matrix (ECM) and cytokines (1). It is well recognised that multiple cell types, such as chondrocytes, osteoblasts, endothelial cells, osteocytes and even mesenchymal stem cells, are involved in bone regeneration via the secretion of growth factors and the temporal expression of bone healing-related genes, such as bone sialoprotein and osteocalcin (3).

Osteocytes are the most common functional cell type involved in fracture healing (4,5). Osteocytes connect with each other and with other cell types, such as osteoblasts, bone marrow cells and periosteal cells, through an abundant dendritic network, which allows migration of signalling factors among the cells (4). Therefore, the position and status of osteocytes are critical for bone metabolism, remodelling and generation (6).

Extracellular signal-regulated kinase (ERK) is a critical regulator of animal development (7). ERK activation initiates a phosphorylation cascade within cells, affects gene expression and causes changes in cell phenotypes, such as proliferation, differentiation and motility (7). Oxidative stress causes decreased autophagy of osteocytes, during which inhibition of ERK signalling impairs autophagosome formation and promotes osteocyte cell death (8). In addition, activation of ERK signalling in osteocytes can cause changes in the cytoskeleton, remodelling of the ECM, and further alteration of tissue structure and bones (1).

The regulator of G protein signalling (RGS) family contains key cytosolic proteins that are capable of accelerating GTPase activity and regulating downstream signalling under various

physiological conditions (9). For example, RGS18 is associated with platelet production and reactivity, and participates in the haemostatic response after injury (10). Plasma levels of RGS18 are a promising biomarker of gastric cancer (11). Furthermore, RGS18 suppresses osteoclastogenesis by negatively regulating OGR1/NFAT signalling in osteoclasts (12). The present study conducted a bioinformatics analysis of acutely injured subjects (AIS) and screened for elevated *RGS18* expression. Gene Set Enrichment Analysis (GSEA) and subsequent experimental verification revealed that ERK signalling is involved in osteocyte proliferation and apoptosis. The present study provides a novel target for bone fracture healing.

Materials and methods

Bioinformatics analysis. The GSE93138 and GSE93215 datasets (13) in the Gene Expression Omnibus (GEO) database (http://www.ncbi.nlm.nih.gov/geo/) were selected for the present bioinformatics analysis. Differentially expressed genes were screened using the 'limma' package (14). In the two datasets, peripheral blood samples were obtained from acutely injured subjects (AIS) collected over multiple days, and were compared with those obtained from age- and sex-matched healthy volunteers (HVs). Microarrays were then performed to compare changes in gene expression between the AIS and HVs. The AIS were enrolled upon presentation for fracture care. To comprehensively analyse the basic functions and participating pathways of the differentially expressed genes, GSEA was performed using GSEA software (version 4.2.1; https://www.gsea-msigdb.org/gsea/index.jsp) with the c2.cp.kegg.v7.1.symbols.gmt gene set (https://www.gsea-msigdb.org/gsea/index.jsp) (15,16).

Specimen selection. All experiments were performed with the approval of the Ethics Committee of The Fifth Affiliated Hospital Jinan University (approval no. 2022-10.19.1.0; Heyuan, China). Peripheral blood samples were collected from AIS (<7 days after injury) (n=10). In total, samples were collected from five male patients and five female patients, with a median age of 43.4 years (range, 26-54 years). The inclusion criterion was patients aged between 18 and 55 years. The exclusion criteria were: Prior knee injury or surgery in either knee, posterior cruciate ligament injury, posterolateral corner injury, lateral collateral ligament injury, diabetes or other systemic diseases, and a history of inflammatory arthritis or gout. Peripheral blood samples were also collected from age- and sex-matched HVs (n=10), and were used as controls. The peripheral blood samples were collected between November 2022 and March 2023. The expression levels of RGS18 were determined by reverse transcription-quantitative PCR (RT-qPCR). All donors signed an informed consent form.

Cell culture. Mouse osteocyte MLO-Y4 cells (Procell Life Science & Technology Co., Ltd.) were cultured in α-minimal essential medium (α-MEM; Procell Life Science & Technology Co., Ltd.) containing 10% foetal bovine serum (FBS; Shanghai Basal Media Technologies Co., Ltd.) and 1% penicillin-streptomycin. Mouse osteoblast MC3T3-E1 cells (Nanjing Cobioer Biosciences Co., Ltd.) were cultured in α-MEM containing 20% FBS, 2 mM L-glutamine, 1 mM sodium pyruvate,

and 1% penicillin-streptomycin. The cells were maintained at 37˚C in an incubator containing 5% CO_2 and 95% humidity. The ERK activator 12-O-tetradecanoylphorbol-13-acetate (TPA) and MEK1/2 inhibitor PD98059 were purchased from MilliporeSigma.

RT-qPCR. Total RNA was extracted from the collected peripheral blood samples and MLO-Y4 and MC3T3-E1 cells using Trizol reagent (Beyotime Institute of Biotechnology). RNA then underwent cDNA synthesis using a Prime Script RT-PCR kit (Takara Biotechnology Co., Ltd.) according to the manufacturer's protocol. TB Green Fast qPCR Mix (Takara Biotechnology Co., Ltd.) was used for qPCR. The following thermocycling conditions were used: 95˚C for 30 sec, followed by 40 cycles at 95˚C for 5 sec and 60˚C for 10 sec. The expression levels of genes were normalised to *GAPDH* using the $2^{-\Delta\Delta Cq}$ method (17). The primer sequences were designed and synthesised by Shanghai GenePharma Co., Ltd., as follows: Mouse *RGS18*, forward 5'-GGCCAAAGAAACAAGATGGAGT-3', reverse 5'-ACACTCTGCTTTGTGCCGTA-3'; mouse *GAPDH*, forward 5'-CAGGAGAGTGTTTCCTCGTCC-3', reverse 5'-GATGGGCTTCCCGTTGATGA-3'; human *RGS18*, forward 5'-GCAGAGACAGAAAGAAACGCAG-3', reverse 5'-CTCTTCAGGGGAGACTCTTGT-3'; and human *GAPDH*, forward 5'-CCATGTTGCAACCGGGAAG-3' and reverse 5'-GCCCAATACGACCAAATCAGAG-3'.

Cell transfection. Small interfering RNA (siRNA) targeting *RGS18* (si-RGS18) and a plasmid overexpressing *RGS18* (pcDNA-RGS18) were synthesised by Shanghai GenePharma Co., Ltd. Scrambled siRNA (si-NC) and empty pcDNA3.1 vector were used as negative controls, respectively. The siRNA sequences were as follows: si-RGS18, sense 5'-GGAGAGACUCAAGCCAGUAGA-3', antisense 5'-UCUACUGGCUUGAGUCUCUCC-3'; and si-NC, sense 5'-GAGACAGGGCAGCCAAGUAUA-3' and antisense 5'-UAUACUUGGCUGCCCUGUCUC-3'. For transfection, MLO-Y4 and MC3T3-E1cells were seeded in six-well plates at a density of 5x10⁵ cells/well. A total of 5 μl Lipofectamine™ 2000 (Invitrogen; Thermo Fisher Scientific, Inc.) and 2 μg vectors or 100 nM siRNAs was mixed in 100 μl Opti-MEM™ (Gibco; Thermo Fisher Scientific, Inc.) and added to each well. After 48 h of incubation at 37˚C, the medium was replaced with fresh medium and the cells were cultured for another 24 h.

Cell counting kit 8 (CCK-8) assay. Post-transfection with si-RGS18 or pcDNA-RGS18, MLO-Y4 and MC3T3-E1 cells were seeded into 96-well plates at a density of 5,000 cells/well. After incubation for 12, 24, 48 and 72 h at 37˚C, CCK-8 solution (Thermo Fisher Scientific, Inc.) was added and incubated for a further 2 h. Absorbance was measured at an optical density of 450 nm using a microplate detector (Thermo Fisher Scientific, Inc.).

5-Ethynyl-2'-deoxyuridine (EdU) assay. Following transfection, the proliferation of MLO-Y4 and MC3T3-E1 cells was determined using an EdU assay kit (Beyotime Institute of Biotechnology) according to the manufacturer's instructions. Briefly, MLO-Y4 and MC3T3-E1 cells (5x10³ cells/well in 96-well plates) were stained with EdU (10 μM) at room
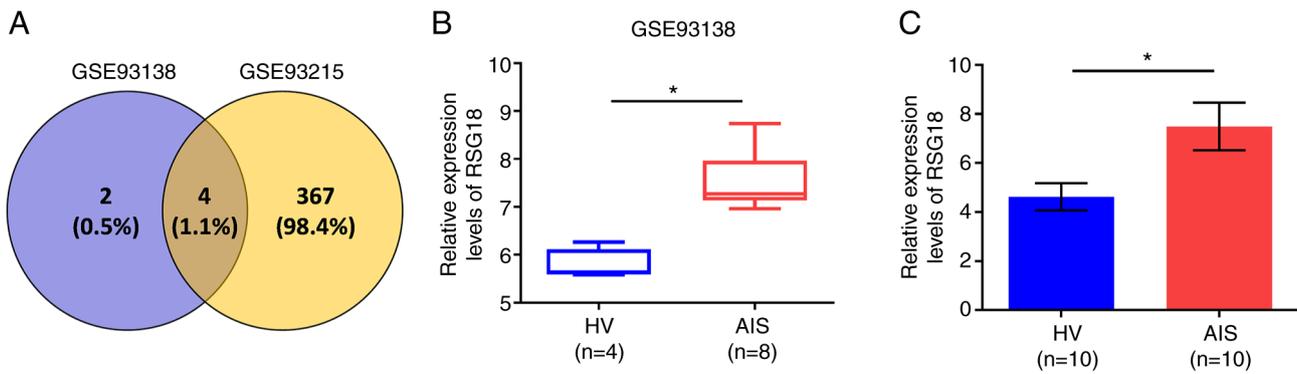
Figure 1. RGS18 expression is increased in samples from AIS. (A) Screening of AIS-related genes using the Gene Expression Omnibus database. (B) *RGS18* was upregulated in samples from AIS compared with those from HVs from the GSE93138 dataset. (C) Reverse transcription-quantitative PCR evaluation of *RGS18* in collected peripheral blood samples. *P<0.05. AIS, acutely injured subjects; HV, healthy volunteer; RGS18, regulator of G protein signalling 18.

temperature for 1 h and then fixed in 4% formaldehyde for 15 min at room temperature (23±2°C), and permeabilised with 0.5% Triton X-100 for 10 min at room temperature. DAPI (Invitrogen; Thermo Fisher Scientific, Inc.) was used to label the nuclei for 20 min at room temperature. Images were captured using a fluorescence microscope (Leica Microsystems, Inc.).

Flow cytometry. Cell cycle arrest and apoptosis were assessed by flow cytometry. Briefly, MLO-Y4 and MC3T3-E1 cells were transfected with si-RGS18 or pcDNA-RGS18 as indicated, followed by treatment with 20 μM PD98059 or 200 nM TPA for 24 h at 37°C. For cell cycle analysis, $1x10^6$ cells were collected and fixed in ice-cold 70% ethanol for 12 h at 4°C and then stained with a mixture of PI (50 μg/ml), 1% Triton-X100 (1%) and DNase-free RNase (100 μg/ml) at 4°C for 30 min. To assess apoptosis, $1x10^5$ cells were collected and stained using an Annexin V-FITC/PI double staining kit (Beyotime Institute of Biotechnology), according to the manufacturer's protocol. The samples were then assessed by flow cytometry (Accuri-C6™ plus; BD Biosciences) and the data were analysed using FlowJo™ software (v7.6.5; FlowJo, LLC).

Western blotting. Total protein lysates were extracted from MLO-Y4 and MC3T3-E1 cells following transfection using RIPA lysis buffer (Beijing Solarbio Science & Technology Co., Ltd.) and were quantified using a BCA kit (Beyotime Institute of Biotechnology). Equal amounts of protein (30 μg) were separated by SDS-PAGE on 10-12% gels and transferred onto nitrocellulose membranes. After blocking with 5% non-fat milk at room temperature for 1 h, the membranes were probed using primary antibodies against RGS18 (cat. no. 11866-1-AP; Proteintech Group, Inc.), cyclin D (cat. no. ab239794; Abcam), cyclin E (cat. no. ab33911; Abcam), cleaved caspase-3 (cat. no. ab32042; Abcam), cleaved caspase-9 (cat. no. 9509; Cell Signaling Technology, Inc/), ERK1/2 (cat. no. ab17942; Abcam), phosphorylated (p)-ERK1/2 (cat. no. ab201015; Abcam), p38 (cat. no. ab170099; Abcam), p-p38 (cat. no. ab236527; Abcam), JNK1/2 (cat. no. ab112501; Abcam), p-JNK1/2 (cat. no. ab4821; Abcam), ERK5 (cat. no. ab196609; Abcam), p-ERK5 (cat. no. ab5686; Abcam) (all 1:1,000) and GAPDH (cat. no. 60004-1-Ig; 1:50,000; Proteintech Group, Inc.) overnight at 4°C. The membranes were then incubated with the corresponding secondary anti-mouse or anti-rabbit antibodies

conjugated to HRP (cat. nos. ab6789 and ab205718; both 1:2,000; Abcam) at room temperature for 1 h. Protein bands of interest were visualised by incubation with an enhanced chemiluminescence reagent (Pierce; Thermo Fisher Scientific, Inc.).

Immunostaining. MLO-Y4 and MC3T3-E1 cells were seeded in confocal dishes at a density of 100,000 cells/well, followed by transfection with si-RGS18 or pcDNA-RGS18. The cells were then washed with PBS, fixed in 4% paraformaldehyde at room temperature for 15 min, permeabilised with 0.5% Triton X-100 at room temperature for 10 min, blocked with 5% BSA at room temperature for 1 h and incubated with a primary antibody against p-ERK1/2 (cat. no. ab201015; 1:200; Abcam) at 4°C overnight. Subsequently, the cells were washed with PBS and incubated with a goat anti-rabbit IgG antibody (Alexa Fluor® 555) (cat. no. ab150078; 1:200; Abcam) and with DAPI for 10 min at room temperature. Five random stained areas were observed under a fluorescence microscope (Leica Microsystems, Inc.).

Statistical analysis. All experiments were repeated three times and all data are presented as the mean ± standard deviation and were analysed using GraphPad Prism 9.5.1 software (Dotmatics). Statistical differences between two groups were measured using unpaired Student's t-test, and differences among three or more groups were analysed using one-way or two-way ANOVA followed by the Bonferroni post hoc test. P<0.05 was considered to indicate a statistically significant difference.

Results

RGS18 expression is increased in AIS. To identify the potential factors associated with bone fracture, gene expression in AIS and HVs from the GSE93138 and GSE93215 datasets of the GEO database was analysed. The overlap analysis identified four genes: *KIAA0825*, *ANXA3*, *RGS18* and *LIPN* that were upregulated in AIS compared with in HVs (Fig. 1A). Given that a previous study reported that RGS18 can impair osteoclast formation (12), *RGS18* was selected for further investigation. Further experiments confirmed that the expression levels of *RGS18* were increased in AIS compared with those in HVs from the GSE93138 dataset (Fig. 1B) and clinical samples (Fig. 1C).
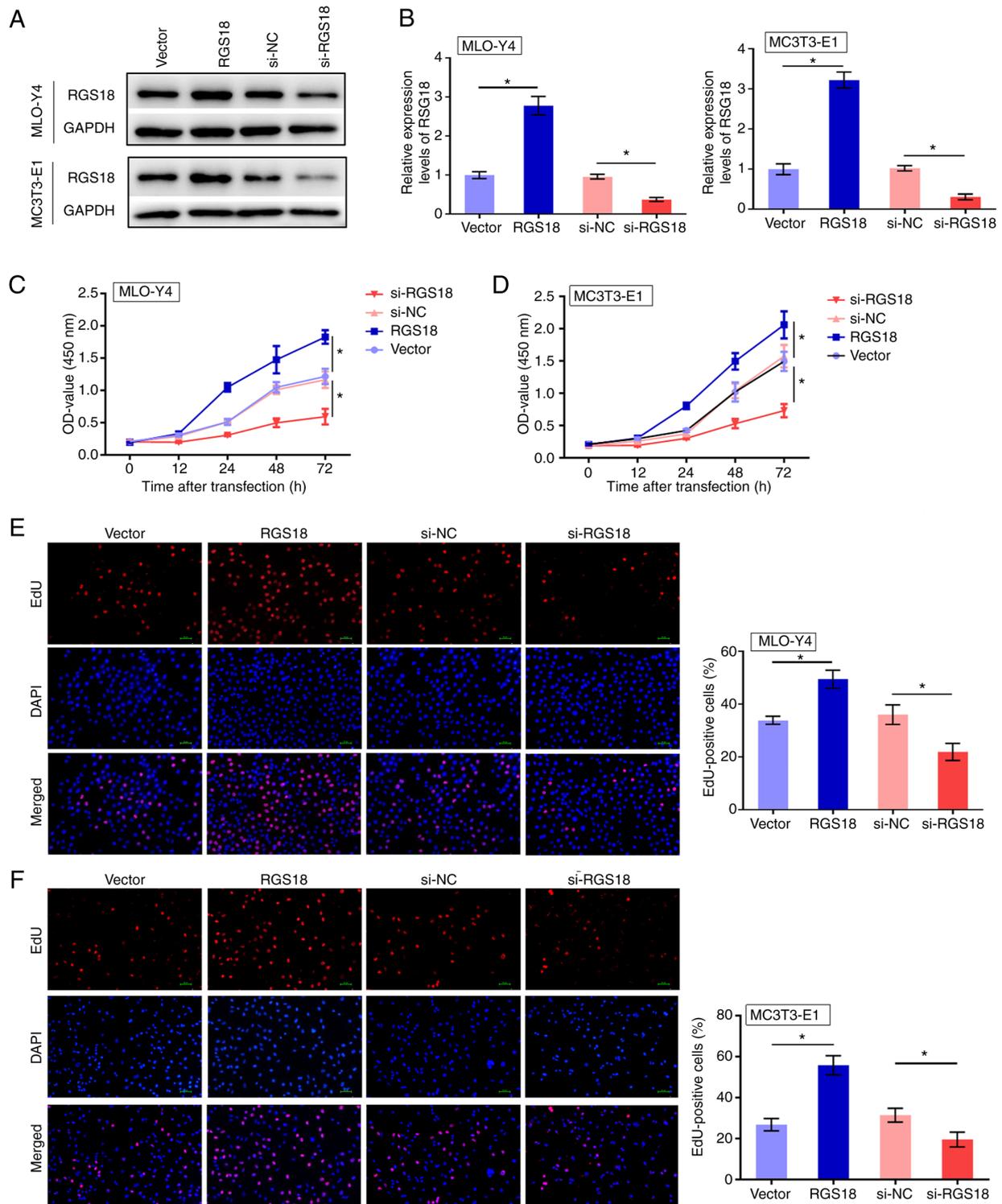
Figure 2. RGS18 promotes the proliferation of osteocytes. (A) Western blotting and (B) reverse transcription-quantitative PCR were performed to detect the expression levels of RGS18 in MLO-Y4 and MC3T3-E1 cells after overexpression or knockdown of *RGS18*. Viability of (C) MLO-Y4 and (D) MC3T3-E1 cells after overexpression or knockdown of *RGS18*, as determined by Cell Counting Kit 8 assay. Proliferation of (E) MLO-Y4 and (F) MC3T3-E1 cells after overexpression or knockdown of *RGS18*, as determined by EdU staining (magnification, x200). *P<0.05. EdU, 5-ethynyl-2'-deoxyuridine; NC, negative control; OD, optical density; RGS18, regulator of G protein signalling 18; si, small interfering.

RGS18 promotes osteoclast viability and proliferation. To assess the function of RGS18 in bone fracture, MLO-Y4 and MC3T3-E1 osteocytes were transfected with *RGS18* overexpression vector or *RGS18* siRNA, and the transfection efficiency was validated by western blot analysis and RT-qPCR (Fig. 2A and B). The viability of MLO-Y4 and

MC3T3-E1 cells was promoted by *RGS18* overexpression, but was suppressed by *RGS18* knockdown (Fig. 2C and D). Furthermore, overexpression of *RGS18* increased and silencing of *RGS18* decreased the number of EdU-positive MLO-Y4 and MC3T3-E1 cells (Fig. 2E and F), thus indicating that RGS18 contributes to osteocyte proliferation.
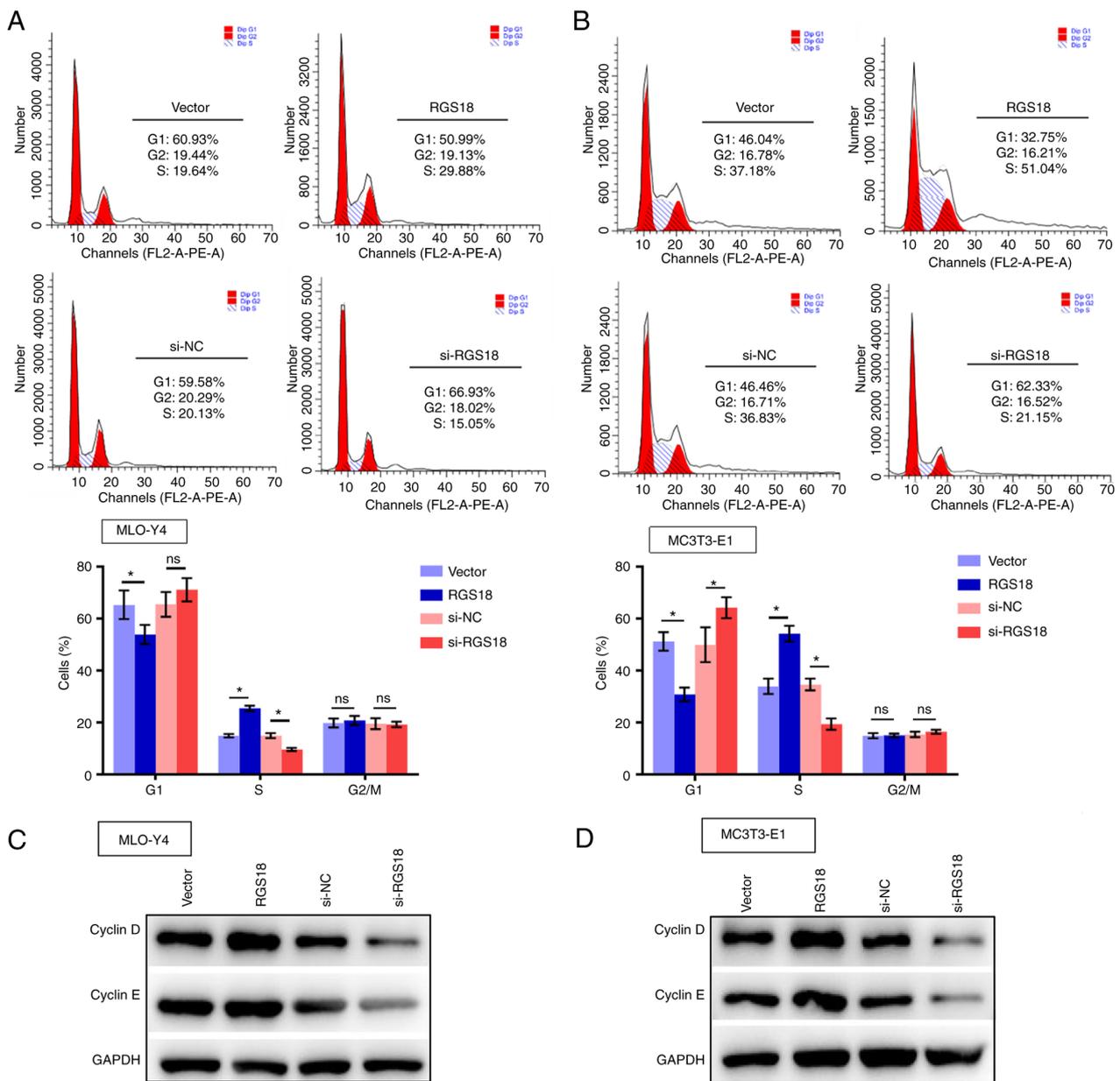
Figure 3. RGS18 promotes the cell cycle progression of osteocytes. Flow cytometry was performed to detect cell cycle progression of (A) MLO-Y4 and (B) MC3T3-E1 cells after overexpression or knockdown of *RGS18*. Western blotting was conducted to detect the expression levels of cell cycle-associated proteins in (C) MLO-Y4 and (D) MC3T3-E1 cells after overexpression or knockdown of *RGS18*. ns, not significant; $^{*}P<0.05$. NC, negative control; RGS18, regulator of G protein signalling 18; si, small interfering.

RGS18 promotes osteocyte cell cycle progression. The present study then examined the effect of RGS18 on osteocyte cell cycle progression. It was revealed that overexpression of *RGS18* reduced the population of MLO-Y4 and MC3T3-E1 cells in G_1 phase, but increased the number of cells in S phase (Fig. 3A and B). By contrast, the number of MLO-Y4 and MC3T3-E1 cells in S phase was decreased by *RGS18* knockdown (Fig. 3A and B). Furthermore, the expression levels of cell cycle-related proteins cyclin D and cyclin E were increased by *RGS18* overexpression but decreased by *RGS18* knockdown in MLO-Y4 and MC3T3-E1 cells (Fig. 3C and D), implying that RGS18 contributes to osteocyte cell cycle progression.

RGS18 suppresses osteocyte apoptosis. The present study also evaluated the function of RGS18 in modulating osteocyte apoptosis (early + late) and necrosis. Notably, apoptosis and necrosis of MLO-Y4 and MC3T3-E1 cells was suppressed by *RGS18* overexpression, but enhanced by *RGS18* knockdown (Fig. 4A and B). In addition, the expression levels of apoptosis-related proteins cleaved caspase-3 and cleaved caspase-9 were inhibited by *RGS18* overexpression and enhanced by *RGS18* knockdown in MLO-Y4 and MC3T3-E1 cells (Fig. 4C and D), indicating that RGS18 may suppress osteocyte apoptosis.

RGS18 stimulates MAPK signalling. The present study explored the potential mechanisms underlying RGS18-mediated osteocyte function. GSEA of the GSE93138 dataset identified MAPK signalling as one of the RGS18-stimulated signalling pathways (Fig. 5A). Considering MAPK signalling is a critical
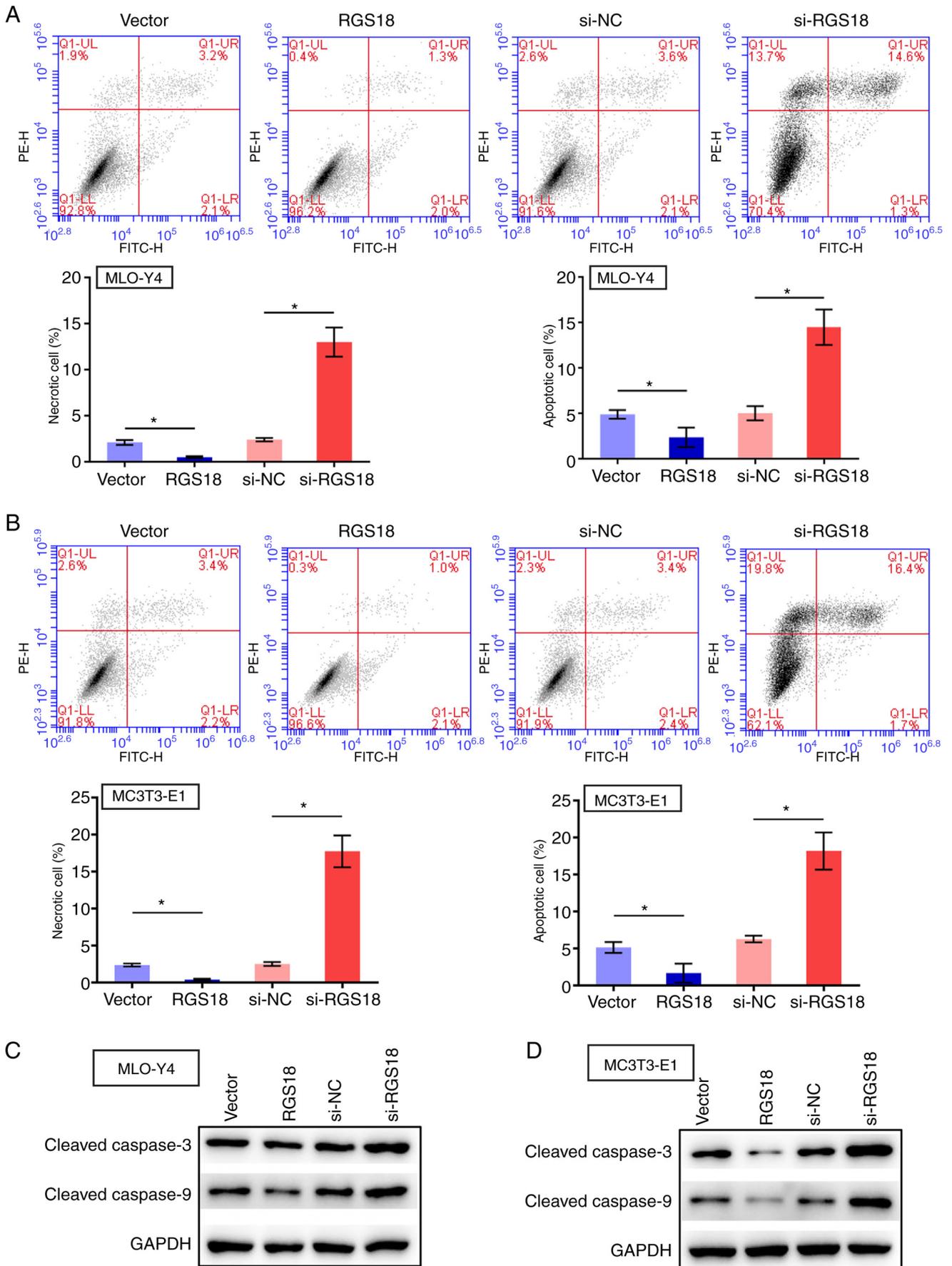
Figure 4. RGS18 suppresses apoptosis of osteocytes. Flow cytometry was performed to detect the proportions of apoptotic and necrotic (A) MLO-Y4 and (B) MC3T3-E1 cells after overexpression or knockdown of *RGS18*. Western blotting was conducted to detect the expression levels of apoptotic proteins in (C) MLO-Y4 and (D) MC3T3-E1 cells after overexpression or knockdown of *RGS18*. *P<0.05. NC, negative control; RGS18, regulator of G protein signalling 18; si, small interfering.
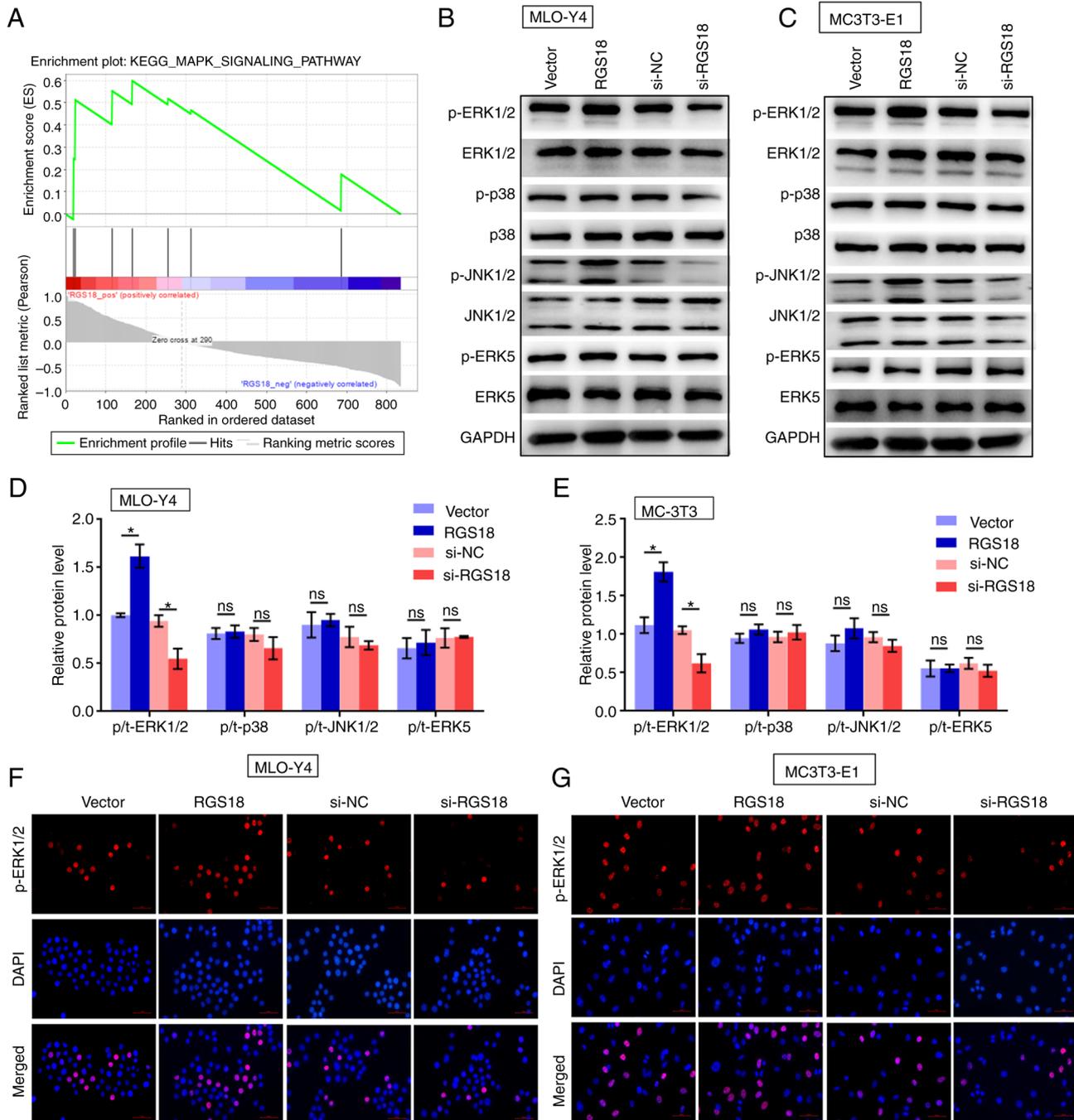
Figure 5. RGS18 stimulates MAPK signalling. (A) Gene Set Enrichment Analysis of RGS18-activated signalling pathways. Expression levels of ERK signalling pathway-related proteins in (B) MLO-Y4 and (C) MC3T3-E1 cells after overexpression or knockdown of *RGS18* were detected by western blotting. Quantitative analysis results of the expression of ERK signalling pathway-related proteins in (D) MLO-Y4 and (E) MC3T3-E1 cells. Immunofluorescence staining of p-ERK in (F) MLO-Y4 and (G) MC3T3-E1 cells (magnification, x400). *P<0.05. ERK, extracellular signal-regulated kinas; NC, negative control; ns, not significant; p-, phosphorylated; RGS18, regulator of G protein signalling 18; si, small interfering.

signalling pathway that is activated due to mechanical stimuli, and results in osteocyte cytoskeletal changes and ECM remodelling (1), MAPK signalling was selected for further analysis. Phosphorylation of ERK1/2, but not of p38, JNK1/2 or ERK5, was induced by *RGS18* overexpression and was inhibited by *RGS18* knockdown in MLO-Y4 and MC3T3-E1 cells (Fig. 5B-E). Immunofluorescence analysis confirmed that the levels of p-ERK1/2 were enhanced by *RGS18* overexpression and reduced by *RGS18* knockdown in MLO-Y4 and MC3T3-E1 cells (Fig. 5F and G).

RGS18 promotes osteocyte proliferation through ERK signalling. The present study evaluated the association between RGS18 and ERK signalling in the modulation of osteocyte proliferation. EdU-positive MC3T3-E1 cells were enhanced by *RGS18* overexpression, whereas treatment with the MEK1/2 inhibitor PD98059 blocked this effect (Fig. 6A). Furthermore, overexpression of *RGS18* attenuated the proportion of MC3T3-E1 cells in G_1 phase, but enhanced the number of MC3T3-E1 cells in S phase, whereas PD98059 reversed this effect (Fig. 6B). In addition, overexpression of *RGS18* suppressed MC3T3-E1 cell apoptosis and necrosis,
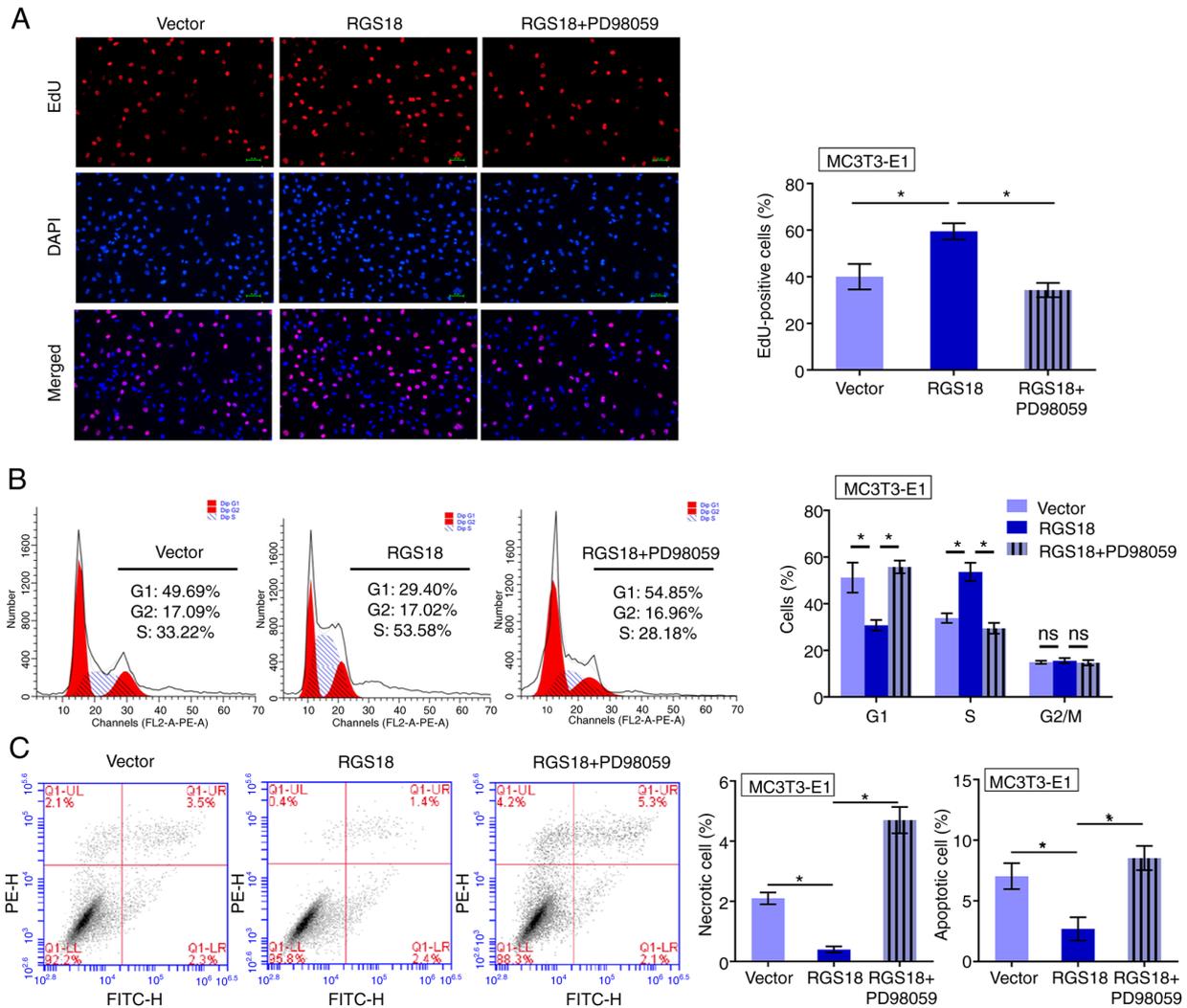
Figure 6. RGS18 promotes the proliferation of osteocytes through ERK signalling. MC3T3-E1 cells with *RGS18* overexpression were treated with or without the ERK inhibitor PD98059 (20 μM). (A) Proliferation of MC3T3-E1 cells was determined by EdU staining (magnification, x200). (B) Cell cycle progression, and (C) apoptosis and necrosis of MC3T3-E1 cells were detected by flow cytometry. *P<0.05. EdU, 5-ethynyl-2'-deoxyuridine; ERK, extracellular signal-regulated kinas; RGS18, regulator of G protein signalling 18.

whereas treatment with PD98059 reversed this effect (Fig. 6C). Collectively, these data indicated that RGS18 contributes to osteocyte proliferation by activating ERK signalling.

ERK activation reverses RGS18 knockdown-induced osteocyte death. The present study observed that knockdown of *RGS18* decreased the number of EdU-positive MC3T3-E1 cells, whereas treatment with the ERK1/2 activator TPA reversed this effect (Fig. 7A). The distribution of MC3T3-E1 cells in G_1 phase was enhanced, but the number of MC3T3-E1 cells in S phase was reduced by *RGS18* knockdown, whereas TPA treatment reversed these effects (Fig. 7B). In addition, the apoptosis and necrosis of MC3T3-E1 cells was promoted by *RGS18* knockdown, whereas treatment with TPA blocked this effect (Fig. 7C), thus indicating that ERK activation reversed *RGS18* knockdown-induced osteocyte death.

Discussion

Bone fracture healing is a complex regenerative process involving various cells, such as chondrocytes, osteoblasts,

endothelial cells and mesenchymal stem cells, and released factors, such as bone sialoprotein and osteocalcin (3). Osteocytes serve a crucial role in the modulation of metabolism, remodelling and bone generation during fracture healing. In the present study, the role of RGS18 in the regulation of bone fractures and osteocytes was uncovered.

RGS18 is a member of the RGS family, and participates in multiple physiological and pathological processes. It has been reported that RGS18 inhibits platelet activation, and induces platelet production and survival (10). RGS18 also functions as a myeloerythroid lineage-related modulator of G protein signalling in megakaryocytes (18). In addition, RGS18 regulates cilia-related mechanosensory processes (19) and serves as a negative modulator of osteoclastogenesis by regulating NFAT signalling (12). In the present study, it was revealed that *RGS18* was more highly expressed in samples from AIS compared with those from HVs. Cell viability and proliferation of osteocytes were promoted by *RGS18* overexpression, but were suppressed by *RGS18* knockdown. Furthermore, overexpression of *RGS18* increased the number of S-phase osteocytes, and *RGS18*
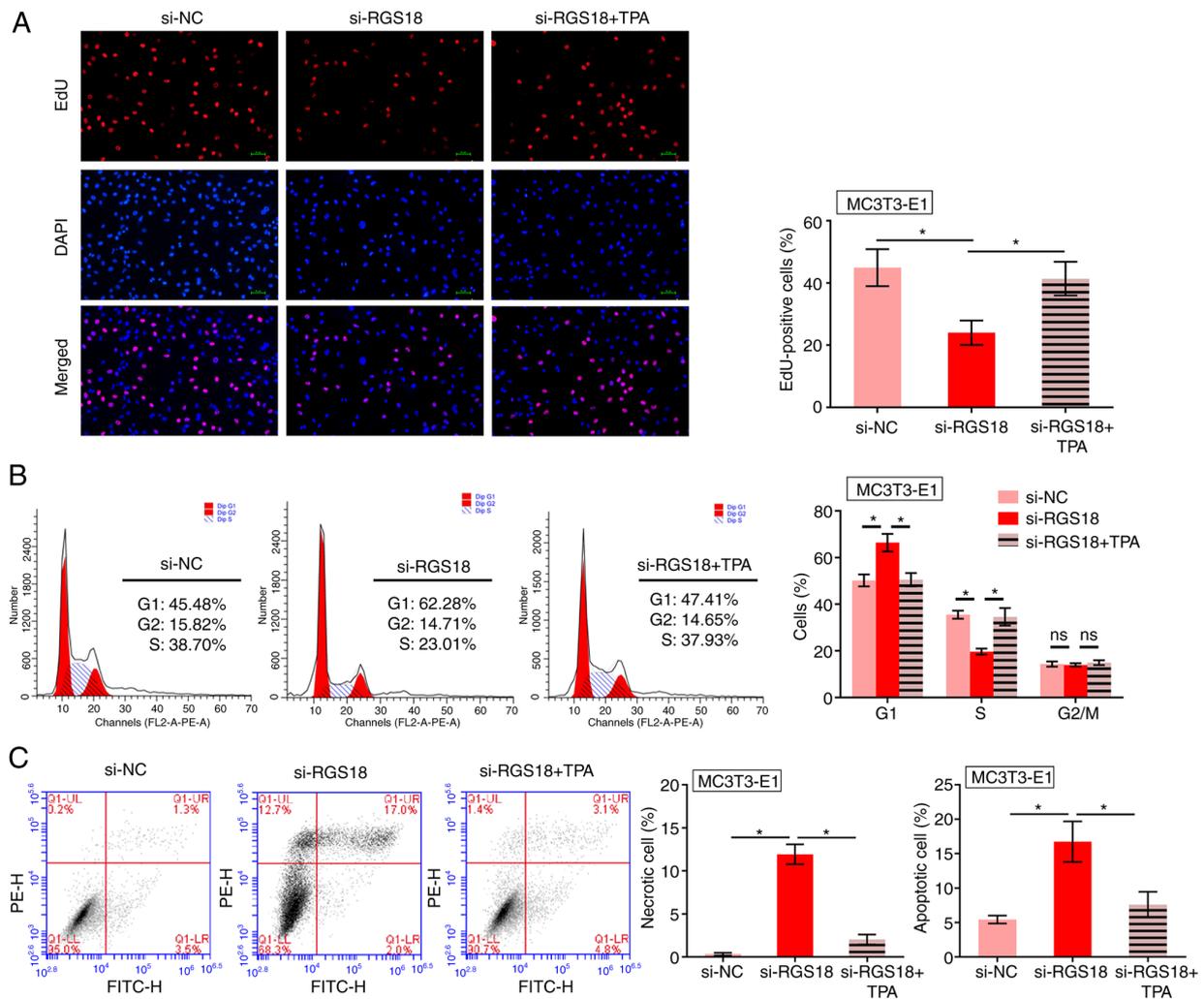
Figure 7. ERK activation reverses *RGS18* knockdown-induced osteocyte death. MC3T3-E1 cells with *RGS18* knockdown were treated with or without ERK activator TPA (200 nM). (A) Proliferation of MC3T3-E1 cells was determined by EdU staining (magnification, x200). (B) Cell cycle progression, and (C) apoptosis and necrosis of MC3T3-E1 cells were detected by flow cytometry. $^*P<0.05$. EdU, 5-ethynyl-2'-deoxyuridine; ERK, extracellular signal-regulated kinas; RGS18, regulator of G protein signalling 18; si, small interfering; TPA, 12-O-tetradecanoylphorbol-13-acetate.

knockdown resulted in the opposite effect. Osteocyte apoptosis was suppressed by *RGS18* overexpression but induced by *RGS18* knockdown. These data suggested that RGS18 contributes to osteocyte proliferation, indicating a potential function of RGS18 in the regulation of bone fracture healing. The present findings elucidate a novel function of RGS18 in bone fracture healing and osteocytes. The effects of RGS18 on bone-fracture healing should be confirmed in future *in vitro* and *in vivo* studies.

Regarding the underlying mechanism, GSEA of the GSE93138 dataset revealed that RGS18 could stimulate MAPK signalling. Phosphorylation of ERK1/2 was induced by *RGS18* overexpression in osteocytes. Furthermore, the present study confirmed that treatment with the MEK1/2 inhibitor PD98059 reversed the *RGS18* overexpression-induced osteocyte proliferation and PD98059 reversed the *RGS18* overexpression-inhibited osteocyte apoptosis. Moreover, the ERK1/2 activator TPA reversed the *RGS18* knockdown-induced suppression of osteocyte proliferation and the *RGS18* knockdown-induced osteocyte apoptosis. These data suggested that RGS18 promotes osteocyte
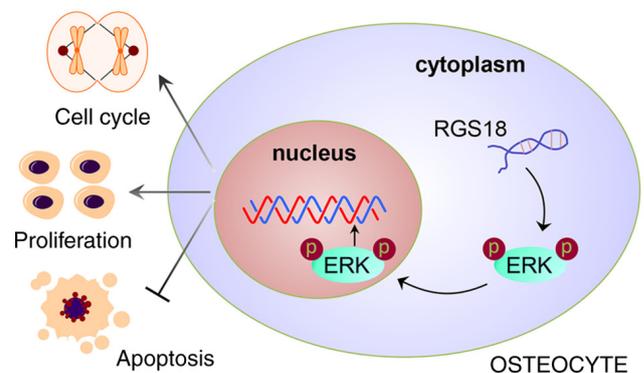

Figure 8. A schematic diagram showing the findings of the present study. RGS18 contributed to the proliferation of osteocytes and bone fracture healing through activating ERK signalling. ERK, extracellular signal-regulated kinas; RGS18, regulator of G protein signalling 18.

proliferation by activating ERK signalling. The present findings provide novel insights into the mechanism by which

RGS18 contributes to bone fracture healing via stimulating ERK signalling. ERK signalling participates in the regulation of osteocyte function during bone fracture healing. It has been reported that HMGB1 contributes to bone fracture healing in a rat tibial fracture model by activating ERK signalling (20). High glucose levels inhibit the expression of connexin 43, and suppress hemichannel function and gap junctions in osteocytes by stimulating ERK signalling (21). Overexpression of *Lgr5* in mesenchymal stem cells promotes fracture healing by modulating mitochondrial dynamics and ERK signalling (22). Furthermore, inhibition of *microRNA-21* can enhance bone fracture healing by activating the ERK pathway (23). These findings suggested that ERK signalling may be one of the mechanisms by which RGS18 mediates bone fracture healing, and other potential mechanisms should be explored to increase the understanding of RGS18-regulated bone fracture healing.

In conclusion, RGS18 may contribute to osteocyte proliferation and bone fracture healing by activating ERK signalling (Fig. 8). RGS18 may be a key factor in promoting osteoblast proliferation, and this study provides a theoretical basis for further development of fracture healing treatments.

Availability of data and materials

The datasets used and/or analysed during the current study are available from the corresponding author on reasonable request. For bioinformatics analysis, the datasets generated and/or analysed during the current study are available in the GEO database (GSE93138: https://www.ncbi.nlm.nih.gov/geo/query/acc.cgi?acc=GSE93138 and GSE93215: https://www.ncbi.nlm.nih.gov/geo/query/acc.cgi?acc=GSE93215).

Authors' contributions

YM conceived and designed the study. YM, SQQ and QW performed experiments. YM and JLZ performed data analysis and interpretation. All authors confirm the authenticity of all the raw data. All authors read and approved the final manuscript.

Ethics approval and consent to participate

The present study follows The Declaration of Helsinki. The protocol of this research was approved by the Ethics Committee of The Fifth Affiliated Hospital Jinan University (ethics approval no. 2022-10.19.1.0). All donors signed informed consent forms.

Patient consent for publication

Not applicable.

Competing interests

The authors declare that they have no competing interests.

References

1. Camal Ruggieri IN, Cícero AM, Issa JPM and Feldman S: Bone fracture healing: Perspectives according to molecular basis. J Bone Miner Metab 39: 311-331, 2021.
2. McBrien CS Jr: Meta-bone fracture repair via minimally invasive plate osteosynthesis. Vet Clin North Am Small Anim Pract 50: 207-212, 2020.
3. Lin X, Patil S, Gao YG and Qian A: The bone extracellular matrix in bone formation and regeneration. Front Pharmacol 11: 757, 2020.
4. Andreev D, Liu M, Weidner D, Kachler K, Faas M, Grüneboom A, Schlötzer-Schrehardt U, Muñoz LE, Steffen U, Grötsch B, *et al*: Osteocyte necrosis triggers osteoclast-mediated bone loss through macrophage-inducible C-type lectin. J Clin Invest 130: 4811-4830, 2020.
5. Choy MHV, Wong RMY, Chow SKH, Li MC, Chim YN, Li TK, Ho WT, Cheng JCY and Cheung WH: How much do we know about the role of osteocytes in different phases of fracture healing? A systematic review. J Orthop Translat 21: 111-121, 2020.
6. Ru JY and Wang YF: Osteocyte apoptosis: The roles and key molecular mechanisms in resorption-related bone diseases. Cell Death Dis 11: 846, 2020.
7. Patel AL and Shvartsman SY: Outstanding questions in developmental ERK signaling. Development 145: dev143818, 2018.
8. Kar R, Riquelme MA, Hua R and Jiang JX: Glucocorticoid-Induced autophagy protects osteocytes against oxidative stress through activation of MAPK/ERK signaling. JBMR Plus 3: e10077, 2019.
9. Masuho I, Balaji S, Muntean BS, Skamangas NK, Chavali S, Tesmer JJG, Babu MM and Martemyanov KA: A global map of G protein signaling regulation by RGS proteins. Cell 183: 503-521 e519, 2020.
10. DeHelian D, Gupta S, Wu J, Thorsheim C, Estevez B, Cooper M, Litts K, Lee-Sundlov MM, Hoffmeister KM, Poncz M, *et al*: RGS10 and RGS18 differentially limit platelet activation, promote platelet production, and prolong platelet survival. Blood 136: 1773-1782, 2020.
11. Su C, Li H, Peng Z, Ke D, Fu H and Zheng X: Identification of plasma RGS18 and PPBP mRNAs as potential biomarkers for gastric cancer using transcriptome arrays. Oncol Lett 17: 247-255, 2019.
12. Iwai K, Koike M, Ohshima S, Miyatake K, Uchiyama Y, Saeki Y and Ishii M: RGS18 acts as a negative regulator of osteoclastogenesis by modulating the acid-sensing OGR1/NFAT signaling pathway. J Bone Miner Res 22: 1612-1620, 2007.
13. McKinley TO, Lisboa FA, Horan AD, Gaski GE and Mehta S: Precision medicine applications to manage multiply injured patients with orthopaedic trauma. J Orthop Trauma 33 (Suppl 6): S25-S29, 2019.
14. Ritchie ME, Phipson B, Wu D, Hu Y, Law CW, Shi W and Smyth GK: limma powers differential expression analyses for RNA-sequencing and microarray studies. Nucleic Acids Res 43: e47, 2015.
15. Subramanian A, Tamayo P, Mootha VK, Mukherjee S, Ebert BL, Gillette MA, Paulovich A, Pomeroy SL, Golub TR, Lander ES and Mesirov JP: Gene set enrichment analysis: A knowledge-based approach for interpreting genome-wide expression profiles. Proc Natl Acad Sci USA 102: 15545-15550, 2005.
16. Mootha VK, Lindgren CM, Eriksson KF, Subramanian A, Sihag S, Lehar J, Puigserver P, Carlsson E, Ridderstråle M, Laurila E, *et al*: PGC-1alpha-responsive genes involved in oxidative phosphorylation are coordinately downregulated in human diabetes. Nat Genet 34: 267-273, 2003.
17. Livak KJ and Schmittgen TD: Analysis of relative gene expression data using real-time quantitative PCR and the 2(-Delta Delta C(T)) method. Methods 25: 402-408, 2001.
18. Yowe D, Weich N, Prabhudas M, Poisson L, Errada P, Kapeller R, Yu K, Faron L, Shen M, Cleary J, *et al*: RGS18 is a myelo-erythroid lineage-specific regulator of G-protein-signalling molecule highly expressed in megakaryocytes. Biochem J 359: 109-118, 2001.

19. Louwette S, Labarque V, Wittevrongel C, Thys C, Metz J, Gijsbers R, Debyser Z, Arnout J, Van Geet C and Freson K: Regulator of G-protein signaling 18 controls megakaryopoiesis and the cilia-mediated vertebrate mechanosensory system. FASEB J 26: 2125-2136, 2012.
20. Chen MQ and Luan JJ: HMGB1 promotes bone fracture healing through activation of ERK signaling pathway in a rat tibial fracture model. Kaohsiung J Med Sci 35: 550-558, 2019.
21. Yang L, Zhou G, Li M, Li Y, Yang L, Fu Q and Tian Y: High glucose downregulates connexin 43 Expression and its gap junction and hemichannel function in osteocyte-like MLO-Y4 cells through activation of the p38MAPK/ERK signal pathway. Diabetes Metab Syndr Obes 13: 545-557, 2020.

22. Lin W, Xu L, Pan Q, Lin S, Feng L, Wang B, Chen S, Li Y, Wang H, Li Y, *et al*: Lgr5-overexpressing mesenchymal stem cells augment fracture healing through regulation of Wnt/ERK signaling pathways and mitochondrial dynamics. FASEB J 33: 8565-8577, 2019.
23. Sheng J, Liang WD, Xun CH, Xu T, Zhang J and Sheng WB: Downregulation of miR-21 promotes tibial fracture healing in rabbits through activating ERK pathway. Eur Rev Med Pharmacol Sci 23: 10204-10210, 2019.